

## Evaluation of Antimicrobial Activity, Brine Shrimp Assay and Anticancer Efficacy (MCF 7 Cell Lines) of *Cinnamomum Zeylanicum* Bark Extract Mediated AgNPs

Supraja N.,<sup>\*a</sup> Rajasekhar K.K.,<sup>b</sup> Kishore B.<sup>c</sup> and Bhavitha J.<sup>b</sup>

<sup>a</sup>Acharya N G Ranga Agricultural University, Institute of Frontier Technology, R.A.R.S, Nanotechnology laboratory, Tirupathi-517507, India.

<sup>b</sup>Department of Pharmaceutical Analysis, Sri Padmavathi School of Pharmacy, Tiruchanoor, Tirupati-517503, India.

<sup>c</sup>Department of Pharmaceutics, Sri Padmavathi School of Pharmacy, Tiruchanoor, Tirupati-517503, India.

\*Corresponding author E-mail address: [krishna.supraja@gmail.com](mailto:krishna.supraja@gmail.com) (Supraja N)

ISSN: 2582-3353



### Publication details

Received: 03<sup>rd</sup> September 2021

Revised: 19<sup>th</sup> October 2021

Accepted: 19<sup>th</sup> October 2021

Published: 02<sup>nd</sup> November 2021

**Abstract:** *Cinnamomum zeylanicum* exhibit potential antimicrobial, antioxidant and antifungal properties. Furthermore, cytotoxic and apoptotic activities of several constituents are been recent addition to its biological properties. In the present study, biosynthesized silver nanoparticles using bark extract of *Cinnamomum zeylanicum* were evaluated for their antibacterial and antifungal activities against scale forming bacteria and fungi in PVC pipelines. The synthesis of nanoparticles was characterized by UV-visible spectroscopy carried out to quantify the formation of silver nanoparticles for localized surface Plasmon resonance (LSPR) at 420nm. Fourier transform infrared spectroscopic (FT-IR) analysis revealed that primary, secondary amine groups in combination with the proteins present in the bark extract are responsible for the reduction and stabilization of the AgNPs. X-ray diffraction (XRD) micrograph indicated the face centered cubic (FCC) structure of the formed AgNPs and morphological studies including size (average size 50nm) were carried out using transmission electron microscopy (TEM). The hydrodynamic diameter (HDD) (60.6nm) and zeta potential (ZP) (10.4mV) were measured using the dynamic light scattering technique (DLS). The antimicrobial activity as prepared silver nanoparticles was tested against Fungal sp, Gram negative and Gram positive bacteria through disc diffusion method. Further, the cytotoxic effects of synthesized AgNPs were evaluated against Human Breast Cancer (MCF 7) cell line.

**Keywords:** AgNPs; Antimicrobial activity; Bark extract of *Cinnamomum zeylanicum*, Brine shrimp assay, MCF7 cell lines

## 1. Introduction

Metal and metal oxide nanoparticles (measured size is less than 100 nm in at least one dimension) were intensely studied due to their unique chemical, physical and biological properties. A considerable quantum of research has been focused on controlling the size and shape, which is crucial in tuning their physical, chemical and optical properties (Coe et al. 2002).<sup>[2]</sup> Various techniques, including chemical and physical means have been employed to prepare metal and their oxide nanoparticles including chemical reduction (Yu 2007),<sup>[13]</sup> electrochemical reduction (Liu and Lin 2004),<sup>[4,5]</sup> photochemical reduction (Mallick et al. 2005)<sup>[6]</sup> and heat evaporation (Smetana et al. 2005).<sup>[10]</sup> In most of the cases, the surface passivating reagents are needed to prevent nanoparticles from aggregation. Unfortunately, many organic surface passivators such as, thiophenol, thiourea, mercapto acetate, etc., are toxic enough to pollute the environment if large scale nanoparticles are produced. Biosynthesis of nanoparticles has received attention due to the growing need to develop environmentally benign technologies in nanoscale materials synthesis. Biosynthesis of metal nanoparticles using microorganisms

(Basavaraja et al. 2008)<sup>[1]</sup> both live and dead microorganisms are gaining importance by virtue of their facile assembly of nanoparticles. Synthesis of nanoparticles using microorganisms or plants can potentially eliminate this problem by making the nanoparticles more bio-compatible. Use of plant extract for the synthesis of nanoparticles could be advantageous over other environmentally benign biological processes by eliminating the elaborate process of maintaining cell cultures. Jose-Yacaman and co-workers (Gardea-Torresdey et al. 2003)<sup>[3]</sup> first reported the formation gold and silver nanoparticles by living plants. Very recently green silver nanoparticles have been synthesized using various natural products like Citrus reticulata, Dioscorea batatas and Alstonia scholaris (Supraja et al. 2018).<sup>[12]</sup>

*Cinnamomum zeylanicum* tree belongs to the family, Lauraceae most noted for its bark, which provides the world with the commonly known culinary spice, cinnamon. Cinnamon has medicinal property and has been used to treat gastrointestinal complaints and other ailments. Cinnamon possesses antiallergenic, anti-inflammatory, anti-ulcerogenic, anti-pyretic, antioxidant, anaesthetic activities (Lin et al. 2003).<sup>[4]</sup> Previous studies have revealed interesting antimicrobial efficacy in essential oils obtained from *C. zeylanicum*

branches and barks (Supraja et al. 2017)<sup>[11]</sup> however there has been a lack of studies focusing on the chemical composition and antimicrobial properties of essential oils obtained from its leaves. This study aimed to analyze the chemical composition of the bark extract obtained from *C. zeylanicum* its inhibitory effect on the bacteria and fungi. However, there are no reports available on antimicrobial activity, Brine shrimp assay and Anti-cancer activity (MCF 7 cell lines) of either aqueous extract of this plant or the silver nanoparticles synthesized using this plant extract.

## 2. Materials and measurements methods

Silver nitrate (>99% pure) was purchased from Sigma Aldrich, India. Potato dextrose broth, Potato dextrose agar, Nutrient broth, Nutrient agar plate, was supplied by Hi-media, India.

### 2.1. Collection of Biofilm formed in poly vinyl chloride (PVC) pipes

The PVC Biofilm samples were collected from four different regions located in and around Tirupati, (Chittoor District) Andhra Pradesh, India. The samples were collected from drinking water supply PVC pipelines and stored in plastic bottles. The collected samples were in amorphous form. These samples were stored in an ice box and transported for further microbiological characterization analysis.

### 2.2. Collection of Plant Material

Healthy plant of *Cinnamomum zeylanicum* was collected from local market and plant bark was collected by scrapping the trunk using neat and clean knife and collected material was carefully washed and dried at 45°C to constant weight. The dried bark was powdered and passed through a BSS no. 85-mesh sieve and stored in air tight container.

### 2.3. Preparation of aqueous extract (AE)

The collected *Cinnamomum zeylanicum* bark was shade dried for 72 h and was ground to get fine powder. Then 10 g of as collected powder was mixed with 100 mL of distilled water and boiled for 30 min. After that the extract was filtered using Whatman No.1 filter paper and collected in plastic bottle and stored at 4°C for further characterization and experimentation.

### 2.4. Isolation of Fungal and Bacterial sp. from drinking water pipeline

Eight fungal species and ten bacterial samples were isolated from drinking water supply PVC pipelines in Tirupati, Chittoor district, AP, India. Through serial dilution pour plate technique, fungal sp. was isolated using Potato Dextrose Agar Medium (PDA) and Gram negative, Positive bacteria was isolated from Nutrient Agar medium. Further it is maintained in Potato Dextrose Agar slants (Fungi) and Nutrient agar slants (Bacteria) for onward analysis. Morphologically dissimilar colonies were selected randomly from all plates and isolated colonies were purified using appropriate medium by streaking methods. Extraction of DNA from Bacterial amplification by using PCR approximately 1300bp of a consensus 16S rRNA gene: forward primer 63f (5<sup>1</sup>-CAG GCC TAA CAC ATG CAA GTC-3<sup>1</sup>) and reverse primer 1387r (5<sup>1</sup>-GGG CGG WGT GTA CAA GGC-3<sup>1</sup>) Primers

27f and 1392r were also used and Fungal genomic DNA was extracted by using the CTAB fungal amplification by using PCR approximately 200-bp with primer ITS-1f (5<sup>1</sup>-CAACTCCCAACCCCTGTGA-3<sup>1</sup>) and reverse primer ITS-4r (5<sup>1</sup>-GCGACGATTACCAGTAACGA-3<sup>1</sup>). Then the pure cultures of bacterial and fungal species were sent to sequence analysis, raw sequences were edited and assembled using the Auto Assembler program (V5.2). All the sequences were used to identify the bacteria and fungi with the help of the BLASTn program <http://www.ncbi.nlm.nih.gov/BLAST>.

### 2.5. Preparation of *Cinnamomum zeylanicum* Silver nanoparticles

To prepare the AgNPs, a 90 mL aqueous solution of 1.0 × 10<sup>-3</sup> M silver nitrate was mixed with a 10 mL of 5% aqueous solution of *Cinnamomum zeylanicum* bark extract. The *Cinnamomum zeylanicum* Ag solution was yellow in color and the solution was stirred repeatedly for an hour and observed that the color of the solution has been changed to dark brown which visually confirms the formation of silver nanoparticles. The initial concentration of the *Cinnamomum zeylanicum* silver nanoparticles was measured using ICP-OES and was found to be 170 ppm. Then, by diluting this solution, each sample of different concentrations was used to investigate the concentration dependence of the antibacterial effect of as prepared Ag nanoparticles and were characterized by using the techniques like, X-ray diffractometry (XRD), Fourier transform infrared spectrophotometry, (FT-IR), UV-Vis spectrophotometry, Dynamic light scattering (Particle size, zeta potential) and Transition electron microscopy (TEM).

### 2.6. Measurement of concentration of AgNPs using inductively coupled plasma optical emission spectrophotometer (ICP-OES)

The concentrations of the *Cinnamomum zeylanicum* bark extract mediated AgNPs were measured using inductively coupled plasma optical emission spectrophotometer (ICP-OES) (Prodigy XP, Leeman labs, USA). The samples were prepared with 10 times dilution after centrifugation at 4000rpm for 15 min. Then 20 ml of aliquot was loaded to the racks of automatic sampler and estimated the concentration of AgNPs thrice and recorded the average concentration.

### 2.7. Assay for antimicrobial activity of *Cinnamomum zeylanicum* silver nanoparticles against microorganisms (Fungi and Bacteria)

The antimicrobial activity of *Cinnamomum zeylanicum* silver nanoparticles was examined on the basis of colony formation by *in vitro* Petri dish assays (Disc diffusion). Each fungal and bacterial isolate was cultured on growth media that induced prolific conidia and bacterial production. The fungus isolates were grown on potato dextrose agar medium and bacterial isolates were grown on nutrient agar medium. Conidia were collected from cultures that were incubated at 37°C for 10 days (Fungi) and Bacterial cultures were collected from cultures that were incubated at 37°C for 2 days for (Bacteria), and diluted with sterile, deionized water to a concentration of 10<sup>6</sup> spores' ml<sup>-1</sup>. Aliquots of the conidial suspension and bacterial suspension were mixed with serial concentrations of

silver preparations to a final volume of 1 ml and were also mixed with sterile, deionized water as control. A 10- $\mu$ l subsample of the conidia and *Cinnamomum zeylanicum* silver mixture stock was taken at 50 $\pm$ 0.9ppm, 100 $\pm$ 1.1ppm and 170 $\pm$ 1.4ppm after silver treatments and diluted 100-fold with the deionized water. A 10- $\mu$ l aliquot of the diluted spore suspension was spread on potato dextrose agar (PDA; Becton, Dickson and Company, Sparks, MD) medium. Three PDA plates for fungi and three NA plates for bacteria per each combination of exposure *Cinnamomum zeylanicum* silver concentration were tested. The filter paper disc dipped in different ppm and inserted on mediums (PDA) then the plates were incubated at 37°C for 2-4 days for fungi and bacteria respectively. The average number of colonies from silver-treated spore suspensions (fungi) and (bacteria) was compared with the number on the water control (percent colony formation). The zone size was determined by measuring the diameter of the zone in mm (Reeves et al. 1999).<sup>[9]</sup>

## 2.8. MTT Assay

Human breast cancer cell line was used to evaluate the percentage of cell inhibition. MCF 7 cells were sub-cultured and seeded, different concentrations (10-50  $\mu$ g/ml) of cytotoxic drug (Synthesized AgNPs) was diluted in maintenance medium (Dulbeccous Modified Eagle Medium) and it was added to each well. After 4 hours, the fresh medium containing MTT dye was add and incubate for 10 hours at 37°C. The medium containing dye was removed and DMSO (Dimethyl sulphoxide) was added to dissolve the formazan crystals. Mitochondrial dehydrogenases of viable cells reduce the yellow water soluble MTT to water insoluble formazan crystals, which were solubilized by DMSO. The absorbance was recorded at 570nm using ELISA reader. Each experiment was done in triplicate (Supraja et al. 2018).<sup>[12]</sup>

**Calculation:** Percentage of cell inhibition (%) = 100 - (Sample absorbance/Control absorbance)  $\times$  100

## 2.9. Brine shrimp lethality assay (BSLA)

Brine shrimp eggs were obtained from the New Aqua Laboratory in Thampanoor, Thiruvananthapuram. Filtered, artificial seawater was prepared by dissolving 35 g of sea salt in 1 litre of distilled water for hatching the shrimp eggs. The seawater was put in a small plastic container (hatching chamber) with a partition for dark (covered) and light areas. Shrimp eggs were added into the dark side of the chamber while the lamp above the other side (light) will attract the hatched shrimp. Three days were allowed for the shrimp to hatch and mature as nauplii (larva). After two days, when the shrimp larvae are ready, 5 mL of the artificial seawater and 5 mL of nanoparticles solution was added to each test tube and 10 brine shrimps were introduced into each tube. Thus, there were a total of 30 shrimps per dilution. The artificial seawater up to 10 mL per test tube is control. The test tubes were left uncovered under the lamp. The number of surviving shrimps were counted and recorded after 24 hrs. Using probit analysis the lethality concentration (LC<sub>50</sub>) was assessed at 95% confidence intervals. LC<sub>50</sub> of less than 100 ppm was considered as potent (active). As mentioned by Meyer and others, LC<sub>50</sub> value of less than 1000  $\mu$ g/mL is toxic while LC<sub>50</sub> value of greater than 1000  $\mu$ g/mL is non-toxic. The percentage mortality (%M) was also calculated by

dividing the number of dead nauplii by the total number, and then multiplied by 100%. This is to ensure that the death (mortality) of the nauplii is attributed to the compounds present in the nanoparticles (Supraja et al. 2018).<sup>[12]</sup>

## 2.10. Characterization of silver nanoparticles

### 2.10.1. Localized surface plasmon resonance (LSPR) - UV – Visible spectroscopy

The bio-reduction of silver ions was monitored by UV-visible spectroscopy at various time intervals. The UV – Visible spectra of this solution was recorded in spectra 2450, SHIMADZU Spectrophotometer, from 200 to 800 nm.

### 2.10.2. FT-IR Analysis for synthesized nanoparticles

The FT-IR spectrum was taken in the mid IR region of 400–4000  $\text{cm}^{-1}$ . The spectrum was recorded using ATR (attenuated total reflectance) technique. The dried sample was mixed with the KBr (1:200) crystal and the spectrum was recorded in the transmittance mode.

### 2.10.3. Particle Size and Zeta potential analyzer for synthesized nanoparticles

The aqueous suspension of the synthesized nanoparticles was filtered through a 0.22 $\mu$ m syringe driven filter unit and the size and distribution of the nanoparticles were measured using Dynamic Light Scattering (DLS) technique (Nanopartica, HORIBA, SZ-100).

### 2.10.4. X-ray Diffraction (XRD) analysis for synthesized nanoparticles

The structure of phyto-reduced silver nanoparticles was revealed by XRD. The XRD pattern was recorded using computer controlled XRD-system (JEOL, and Model: JPX-8030 with CuK $\alpha$  radiation (Ni filtered = 13418  $\text{Å}^0$ ) in the range of 40kV, 20A. The built in software (syn master 7935) program was used for the identification of XRD peaks corresponds to the Bragg's reflections.

### 2.10.5. Transmission Electron Microscopy (TEM)

The surface morphology and size of the nanoparticles was studied by Transmission electron microscopy (JEOL (JEM-1010) instrument) with an accelerating voltage of 80 kV. A drop of aqueous AgNPs on the carbon-coated copper TEM grids were dried and kept under vacuum in desiccators before loading them onto a specimen holder. The particle size and surface morphology of nanoparticles was evaluated using ImageJ 1.45s software.

## 2.11. Statistical analysis

All of the data from three independent replicate trials were subjected to analysis using Statistical package for the Social Sciences (SPSS) version 16.0. The data are reported as the mean + SD and significant differences between mean values were determined with one way analysis of variance (CRD) followed by Duncan's multiple range test (DMRT) (P<0.05).

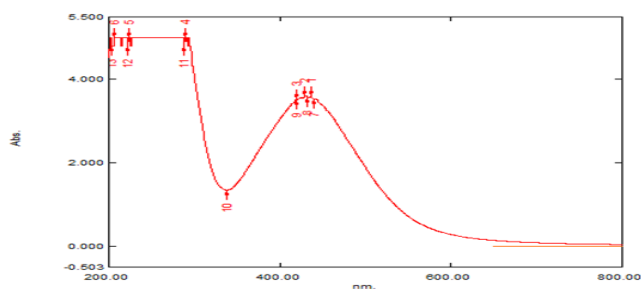


**Fig. 1.** Showing UV-visible spectroscopy recorded using *Cinnamomum zeylanicum* bark extract mediated silver nanoparticles.

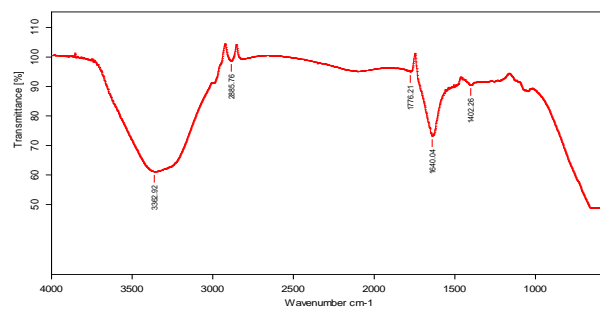


**Fig. 2.** FTIR spectroscopy recorded using *Cinnamomum zeylanicum* bark extract mediated silver nanoparticles.

### 3. Results and Discussions

#### 3.1. Selection of fungi and bacteria present in drinking water pipeline and synthesis of silver nanoparticles

Drinking water pipeline fungi and bacterial species have unusual biological activities depending upon the metabolisms under the influence of temperature, pH and pressure. Once, the bark extract (10ml) was treated with 90ml of silver nitrate solution, the color of the solution changed to dark brown colour Fig. 1 (inset) in less than 5 minutes. The brown color was primarily due to the surface Plasmon resonance of the formed silver nanoparticles.

#### 3.2 UV-Visible spectral analysis – Recording of localized surface plasmon resonance (LSPR) of AgNPs

UV-Visible spectroscopy was employed to understand the biosynthesis of silver nanoparticles by *Cinnamomum zeylanicum*. Fig.1 shows the UV-Visible adsorption spectra of silver nanoparticles after 24hrs incubation at room temperatures (37°C). The spectrum shows peaks at 410 - 460 nm. But the maximum absorbance peak is observed at 420nm under 37°C in 24hrs; the short time enough for the silver ions to silver nanoparticles at 37°C temperature. Silver reduction capacity was observed under UV-Visible adsorption spectroscopy. This shows UV-Vis spectra obtained from solution at room temperature at 7.0 pH. The overall observations suggest that the bio reduction of (silver ions)  $Ag^+$  to  $Ag^{(0)}$  was confirmed by UV-Visible spectroscopy.

#### 3.3. FT-IR analysis – Identification of the bio-molecules responsible for the reduction and stabilization of AgNPs

FT-IR spectrum is used to identify the possible chemical interactions among the silver salts and functional groups present. FT-IR spectrum of the biosynthesized silver nanoparticles using *Cinnamomum zeylanicum* (Fig. 2) shows the absorption peaks at 3362.92, 2886.76, 1776.21, 1540.04 and 1432.35  $cm^{-1}$ . The peak at 3362.92  $cm^{-1}$  reveals the presence of C-H stretching vibration of alkynes, the peak at 2886.76  $cm^{-1}$  indicating the C-H stretching vibrations of alkanes. The peak at 1776.21  $cm^{-1}$  is indicating assigned to the stretching vibration of C=O group of carboxylic acids. The band present at 1540.04  $cm^{-1}$  shows the N-O asymmetric stretching vibration of nitro compounds, the peak present at 1432.35  $cm^{-1}$  indicate stretching vibration of C-H bend alkanes. The FTIR spectra of our dried silver nanoparticles powder show that the carbonyl groups from the amino acid residues

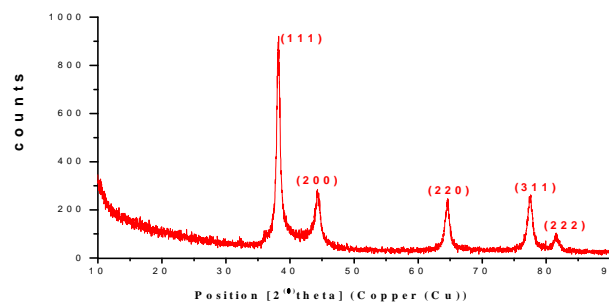


**Fig. 3.** XRD pattern of capped silver nanoparticles synthesized using *Cinnamomum zeylanicum* bark extract mediated silver nanoparticles.

and peptides of proteins have a strong affinity to bind metals. So that protein can act as encapsulating agent and thus protect the nanoparticles from agglomeration. The amide linkages in proteins and polypeptides give well-known signature in IR region. Since a member of C=O group within the cage of cyclic peptides are involved in stabilizing the nanoparticles, the shift of C=O band is quite small. Thus the cyclic peptide plays a crucial role for the reduction of  $Ag^+$  to  $Ag$  as well as stabilizing  $Ag$  nanoparticles.

#### 3.4. X-Ray Diffraction (XRD) analysis

XRD patterns of dried silver nanoparticles synthesized using *Cinnamomum zeylanicum*. A number of Bragg reflections with  $2\theta$  values of 38.03°, 46.18°, 63.43° and 77.18° sets of lattice planes are observed which may be indexed to the (111), (200), (220), (311) and (222) faces of silver respectively Fig. 3. XRD pattern thus clearly illustrates that the silver nanoparticles formed in this present synthesis are crystalline in nature. The crystal phase analysis of face centered cubic (FCC) and then high intensity of 111 plane structure supports the SAED (Selected area electron diffraction) observation results. In addition to the Bragg peaks representative of FCC silver nanoparticles, additional as yet unassigned peaks were also observed suggesting that the crystallization of bioorganic phase occurred on the surface of the nanoparticles. The crystalline size was calculated from the width of the peaks present in the XRD pattern, assuming that they are free from non-uniform strains, using the Debye-Scherrer formula.

$$D = 0.94 \lambda / \beta \cos \theta$$

Where D is the average crystalline domain size perpendicular to the reflecting planes;  $\lambda$  (1.5406  $\times 10^{-10}$ ) is the X-ray wavelength used;

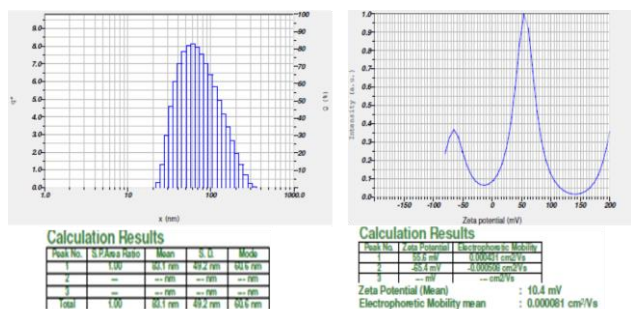


Fig. 4. Showing Dynamic light scattering *Cinnamomum zeylanicum* bark extract mediated silver nanoparticles results showing that particle size and zeta potential.

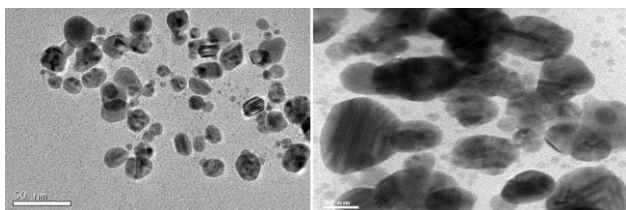


Fig. 5. TEM image of *Cinnamomum zeylanicum* bark extract mediated silver nanoparticles showing spherical shaped particles.

$\beta$  is the full width at half maximum (FWHM) and  $\theta$  is the diffraction angle (Prasad *et al.* 2011).<sup>[7]</sup> The calculated crystalline size of the AgNPs was 50nm.

### 3.5. Dynamic Light scattering analysis

Dynamic Light Scattering analysis measured hydrodynamic diameter of the Ag nanoparticles was found to be 60.6nm Fig. 4a. The recorded value of Zeta potential of the silver nanoparticles was 10.4mV with a single peak Fig. 4b signifies the presence of repulsive electro-static forces among the synthesized silver nanoparticles, which leads to the monodispersity of the particles. If the hydrosol has a large negative or positive zeta potential then they will tend to repel with each other and there will be no tendency of the particles to agglomerate.

### 3.6. TEM analysis

The size and shape of silver nanoparticles using *Cinnamomum zeylanicum* were characterized and shown in the TEM micrograph Fig. 5. It is evident from the micrograph that individual silver nanoparticles as well as a number of aggregates were present and which were spherical in shape with an average particle size of 50nm. The nanoparticles are bound to the functional organic groups (carboxyl and amine) from the *Cinnamomum zeylanicum* bark extract and which may acts template, reducing and stabilizing agents during the synthesis of nanoscale silver particles.

### 3.7. Antimicrobial efficacy of *Cinnamomum zeylanicum* bark extract mediated silver nanoparticles

The prepared silver nanoparticles have very strong inhibitory action against fungal sp, Gram-positive and Gram-negative bacteria Fig. 6 and 7. These isolates were collected from drinking water PVC pipes. Three concentrations of AgNPs (170, 100, 50ppm) were prepared and

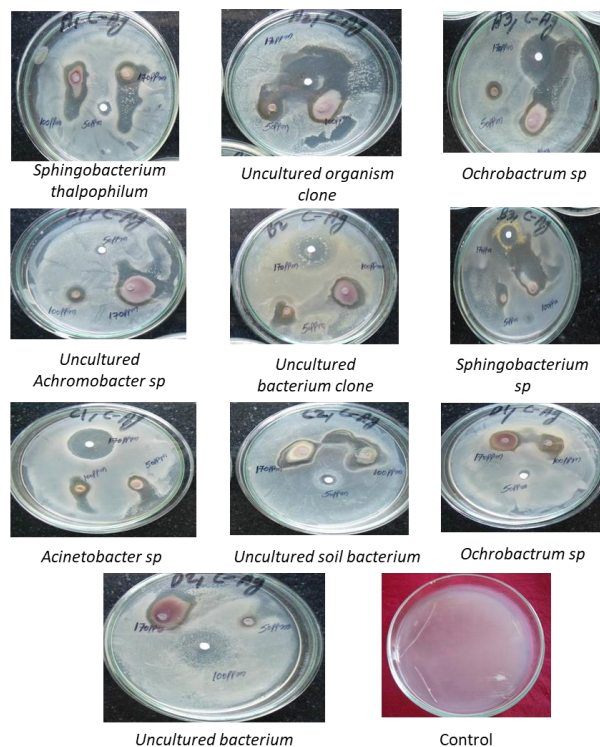


Fig. 6. Synthesized Ag nanoparticles of *Cinnamomum zeylanicum* bark extract showing effective Antibacterial activity towards Gram positive and Gram negative bacteria.

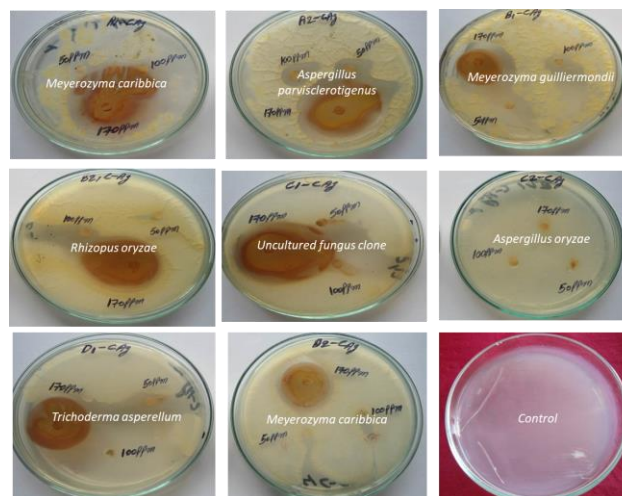


Fig. 7. Synthesized Ag nanoparticles of *Cinnamomum zeylanicum* bark extract showing effective Antifungal activity towards fungal sp.

were applied against an array of fungal species viz, *Meyerozyma caribbica*, *Aspergillus parvisclerotigenus*, *Meyerozyma guilliermondii*, *Rhizopus oryzae*, *Uncultured fungus clone*, *Aspergillus oryzae*, *Trichoderma asperellum* and bacterial species viz., *Spingobacterium thalpophilum*, *Uncultured organism clone*, *Ochrobacterum sp*, *Uncultured Achromobacter sp*, *Uncultured bacterium clone*, *Spingobacterium sp*, *Acinetobacter sp*, *Uncultured soil bacterium*, *Ochrobacterum sp*. Which were isolated from drinking water PVC pipes. The higher concentration (170ppm) of AgNPs showed significant antimicrobial effect Tables 1 and 2 compared with other

**Table 1.** *In-vitro* antibacterial studies of bacteria present in drinking water PVC pipelines using *Cinnamomum zeylanicum* bark extract Silver nanoparticles as inhibitors.

S. no	Bacteria	<i>Cinnamomum zeylanicum</i> bark extract mediated synthesis of silver nanoparticles Zone of inhibition (mm)		
		170±1.4ppm	100±1.1ppm	50±0.9ppm
		1	<i>Sphingobacterium thalophilum</i>	2.5±0.04 <sup>bc</sup>
2	Uncultured organism clone	4.0±0.03 <sup>a</sup>	2.5±0.05 <sup>a</sup>	1.5±0.06 <sup>a</sup>
3	<i>Ochrobactrum</i> sp	3.0±0.05 <sup>a</sup>	2.0±0.04 <sup>abc</sup>	1.0±0.07 <sup>c</sup>
4	Uncultured <i>Achromobacter</i> sp	3.5±0.14 <sup>a</sup>	1.5±0.07 <sup>d</sup>	1.2±0.04 <sup>b</sup>
5	Uncultured bacterium clone	2.5±0.08 <sup>bc</sup>	2.1±0.08 <sup>ab</sup>	0.9±0.05 <sup>cd</sup>
6	<i>Sphingobacterium</i> sp	3.0±0.06 <sup>a</sup>	2.2±0.03 <sup>a</sup>	1.5±0.16 <sup>a</sup>
7	<i>Acinetobacter</i> sp	2.7±0.04 <sup>b</sup>	1.5±0.04 <sup>d</sup>	1.2±0.06 <sup>b</sup>
8	Uncultured soil bacterium	2.0±0.02 <sup>d</sup>	1.9±0.06 <sup>bc</sup>	0.8±0.07 <sup>cd</sup>
9	<i>Ochrobactrum</i> sp	1.7±0.18 <sup>de</sup>	1.5±0.01 <sup>d</sup>	0.6±0.08 <sup>d</sup>
10	Uncultured bacterium	2.2±0.17 <sup>d</sup>	2.0±0.06 <sup>abc</sup>	0.4±0.09 <sup>d</sup>
<b>C.R.D (P&lt;0.05)</b>		<b>0.264</b>	<b>0.214</b>	<b>0.180</b>

Data followed by the same letter are not significantly different at P<0.05, whereas those followed by different letters are significantly different at P<0.05.

**Table 2.** *In-vitro* antifungal studies of fungi present in drinking water PVC pipelines using *Cinnamomum zeylanicum* bark extract of Silver nanoparticles as inhibitors.

S. no	Bacteria	<i>Cinnamomum zeylanicum</i> bark extract of silver nanoparticles Zone of inhibition (mm)		
		170±1.4ppm	100±1.1ppm	50±0.9ppm
		1	<i>Meyerozyma caribbica</i>	2.5±0.12 <sup>b</sup>
2	<i>Aspergillus parvisclerotigenus</i>	1.8±0.14 <sup>c</sup>	1.7±0.22 <sup>c</sup>	1.2±0.05 <sup>a</sup>
3	<i>Meyerozyma guilliermondii</i>	2.3±0.05 <sup>b</sup>	1.4±0.14 <sup>d</sup>	1.2±0.07 <sup>a</sup>
4	<i>Rhizopus oryzae</i>	3.4±0.08 <sup>a</sup>	2.0±0.02 <sup>ab</sup>	0.6±0.08 <sup>c</sup>
5	Uncultured fungus clone	4.0±0.06 <sup>a</sup>	2.0±0.08 <sup>ab</sup>	1.2±0.06 <sup>a</sup>
6	<i>Aspergillus oryzae</i>	1.9±0.04 <sup>c</sup>	1.7±0.06 <sup>c</sup>	1.5±0.04 <sup>a</sup>
7	<i>Trichoderma asperellum</i>	3.0±0.08 <sup>a</sup>	2.2±0.05 <sup>a</sup>	1.0±0.12 <sup>b</sup>
8	<i>Meyerozyma caribbica</i>	2.9±0.02 <sup>a</sup>	1.0±0.04 <sup>d</sup>	0.7±0.14 <sup>c</sup>
<b>C.R.D (P&lt;0.05)</b>		<b>0.280</b>	<b>0.220</b>	<b>0.200</b>

Data followed by the same letter are not significantly different at P<0.05, whereas those followed by different letters are significantly different at P<0.05.

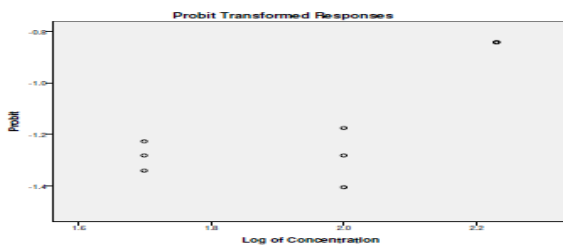


**Fig. 8.** LC<sub>50</sub> (Median Lethal Concentration) values were calculated using the regression line obtained by plotting the concentration against the death percentage on a probit scale, and the results were evaluated with probit analysis (SPSS 13.0).

concentrations (100, 50ppm). The inhibitory action of the microbes may be attributed to the loss of replication ability of DNA upon treatment with the silver ion, besides the fact that expression of ribosomal sub-unit proteins as well as some other cellular proteins and enzymes essential to ATP production becomes inactivated. It is well known that the outer membrane of bacterial cells is predominantly constructed from tightly packed lipopolysaccharide (LPS) molecules, which provide an effective permeability barrier (Raetz 1990).<sup>[8]</sup> We may speculate that a similar mechanism causes the degradation of the membrane structure of bacteria's during treatment with *Cinnamomum zeylanicum* bark extract silver nanoparticles. Extensive investigations directed to better understanding of interaction between silver nanoparticles and bacterial components should shed light on the mode of action of this nanomaterial as a biocidal material.

**Table 3.** Percentage of inhibition measured on MCF 7 cells after the treatment with silver nanoparticles for 48 hours by MTT assay.

Synthesized silver nanoparticles treatment (µg/ml)	Cell inhibition (%)
MCF 7 + 5	19.02%±0.21
MCF 7 + 10	29.08%±0.29
MCF 7 + 20	42.07%±0.02
MCF 7 + 30	65.04%±0.03
MCF 7 + 40	85.06%±0.04
MCF 7 + 50	97.08%±0.05
Control	0.0%

### 3.8. Brine shrimp lethality assay (BSLA)

The prepared silver nanoparticles showed poor brine shrimp larvicidal activity. The lethality concentration (LC<sub>50</sub>) of silver nanoparticles was 50 ppm (µg/mL), 100 ppm, and 170 ppm respectively Fig. 8. The degree of lethality was directly proportional to the concentration of the nanoparticles. Minimum mortalities (30%) were observed at a concentration of 50 ppm while that of 100 and 170 ppm there was no mortality. Based on the results, the brine shrimp lethality of the three different ppm of Ag was found to be concentration-dependent. The observed lethality of the Ag to brine shrimps indicated the presence of potent cytotoxicity. According to these results the AgNPs are slightly toxic (active) if it has an LC<sub>50</sub> value of less than 1000 µg/mL while non-toxic (inactive) if it is greater than 1000 µg/mL.

### 3.9. MTT Assay

The *in-vitro* cytotoxic effects of AgNPs were screened against MCF 7 cell line and the percentage of cell inhibition was confirmed by MTT

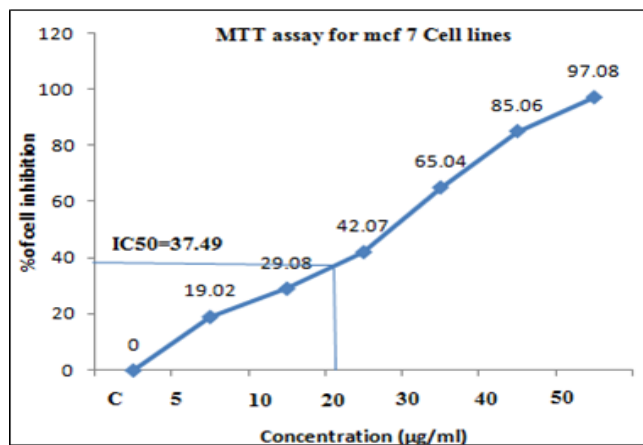


Fig. 9. Cytotoxic activity of *Cinnamomum zeylanicum* bark extract mediated AgNPs against Human breast cancer cell line (MCF7)

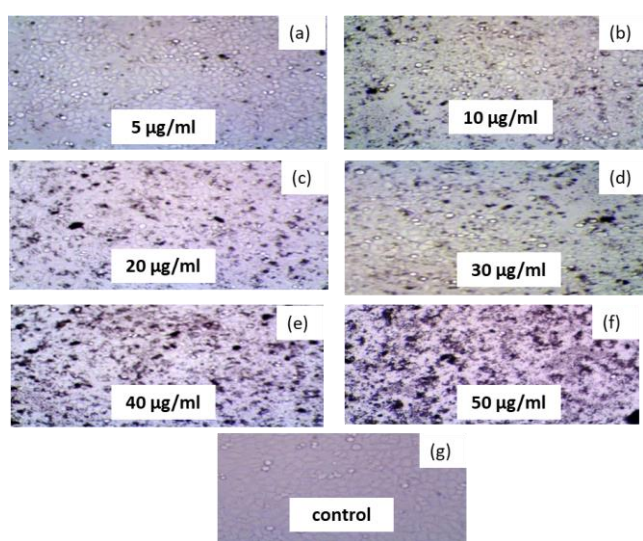


Fig. 10. (a) 5µg/ml, (b) 10 µg/ml, (c) 20 µg/ml, (d) 30 µg/ml, (e) 40 µg/ml, (f) 50 µg/ml, (g) Control shows Breast Cancer Cells (MCF 7) treated with 5-50 µg/ml of synthesized AgNPs using *Cinnamomum zeylanicum* bark extract.

assay Table. 3. The silver nanoparticles were able to inhibit the MCF7 cells in a dose dependent manner (Muthu Irulappan *et al.* 2010).<sup>[14]</sup> After 48 hours of treatment, the AgNPs at concentration of 37.49µg/ml Fig. 9 decreased the viability of MCF 7 cells to 50% of the initial level, Where as in 5 µg/ml treatment of silver nanoparticles shown 19.02% of cell inhibition, 10 µg/ml treatment of silver nanoparticles shown 29.08% of cell inhibition, 20 µg/ml treatment of silver nanoparticles shown 42.07% of cell inhibition, 30 µg/ml treatment of silver nanoparticles shown 65.04% of cell inhibition, 40µg/ml treatment of silver nanoparticles shown 85.06% of cell inhibition, 50 µg/ml treatment of silver nanoparticles shown 97.08% of cell inhibition, and this was chosen as IC<sub>50</sub> Fig. 10. The cytotoxic effects of AgNPs are the active physico-chemical interaction of silver atoms with the functional groups of intracellular proteins, nitrogen bases and phosphate groups in DNA. Although, further studies are needed to fully understanding the mechanism involved in the anticancer activity.

## 4. Conclusions

The synthesis of silver nanoparticles using bark extract *Cinnamomum zeylanicum* can be used as an effective capping as well as reducing agent for the synthesis of silver nanoparticles.

- Silver nanoparticles synthesized by the above method are quite stable; synthesis of metallic nanoparticles using green resources like *Cinnamomum zeylanicum* is a challenging alternative to chemical synthesis, since this novel green synthesis is pollutant free and eco-friendly synthetic rote for silver nanoparticles.
- The result of UV-Vis spectrum, FT-IR, XRD, DLS and TEM has confirmed the bio-reduction of Ag<sup>+</sup> ions.
- The antimicrobial activity of silver nanoparticles synthesized by *Cinnamomum zeylanicum* shown effective results against Fungal sp, Gram positive and Gram negative bacteria and points to the commercial use of these biological synthesized nanoparticles in biomedical and agriculture as fungicides for the effective control of disease causing pathogens.
- While brine shrimp lethality assay elucidates their importance in pharmacological industry, the histogram of % of cell inhibition AgNPs showed excellent cytotoxic effects against MCF 7 cell line in 37.49µg/ml.

## Acknowledgements

Authors are thankful to Acharya N G Ranga Agricultural University for providing research facilities at Institute of Frontier Technology, Regional Agricultural Research Station, Tirupati to carry out this part of the research work.

## Conflicts of Interest

The authors declare no conflict of interest.

## References

- 1 Basavaraja S.; Balaji S.D.; Lagashetty A.; Rajasab A.H.; Venkataraman A. Extracellular Biosynthesis of Silver Nanoparticles using the Fungus *Fusarium semitectum*. *Mater. Res. Bull.*, 2008, **43**, 1164-1170. [\[CrossRef\]](#)
- 2 Coe S.; Woo W.K.; Bawendi M.; Bulović V. Electroluminescence from Single Monolayers of Nanocrystals in Molecular Organic Devices. *Nature*, 2002, **420**, 800-803. [\[CrossRef\]](#)
- 3 Gardea-Torresdey J.L.; Gomez E.; Peralta-Videa J.R.; Parsons J.G.; Troiani H.; Jose-Yacaman M. Alfalfa Sprouts: A Natural Source for the Synthesis of Silver Nanoparticles. *Langmuir*, 2003, **19**, 1357-1361. [\[CrossRef\]](#)
- 4 Lin C.C.; Wu S.J.; Chang C.H.; Ng L.T. Antioxidant Activity of *Cinnamomum cassia*. *Phytother. Res.*, 2003, **17**, 726-730. [\[CrossRef\]](#)
- 5 Liu Y.C.; Lin L.H. New Pathway for the Synthesis of Ultrafine Silver Nanoparticles from Bulk Silver Substrates in Aqueous Solutions by Sonoelectrochemical Methods. *Electrochem. Commun.*, 2004, **6**, 1163-1168. [\[CrossRef\]](#)
- 6 Mallick K.; Witcomb M.J.; Scurrall M.S. Self-Assembly of Silver Nanoparticles in a Polymer Solvent: Formation of a Nanochain through Nanoscale Soldering. *Mater. Chem. Phys.*, 2005, **90**, 221-224. [\[CrossRef\]](#)

- 7 NVKV Prasad T.; Subba Rao Kambala V.; Naidu R. A Critical Review on Biogenic Silver Nanoparticles and their Antimicrobial Activity. *Curr. Nanosci.*, 2011, **7**, 531-544. [[CrossRef](#)]
- 8 Raetz C.R. Bacterial Endotoxins: Extraordinary Lipids that Activate Eucaryotic Signal Transduction. *J. Bacteriol.*, 1993, **175**, 5745-5753. [[CrossRef](#)]
- 9 Reeves D.S.; Wise R.; Andrews J.M.; White L.O. Clinical Antimicrobial Assay, Oxford University Press, New York, USA, 1999. [[Link](#)]
- 10 Smetana A.B.; Klabunde K.J.; Sorensen C.M. Synthesis of Spherical Silver Nanoparticles by Digestive Ripening, Stabilization with various Agents, and their 3-D and 2-D Superlattice Formation. *J. Colloid Interf. Sci.*, 2005, **284**, 521-526. [[CrossRef](#)]
- 11 Supraja N.; TNVKV Prasad. Synthesis, Characterization, and Evaluation of the In-vitro Antimicrobial Efficacy of *Cinnamomum Zeylanicum* Bark-Extract-Mediated. *Res. Med. Eng. Sci.*, 2017, **1**, 000514. [[CrossRef](#)]
- 12 Supraja N.; Prasad T.N.V.K.V.; Gandhi A.D.; Anbumani D.; Kavitha P.; Babujanarthanam R. Synthesis, Characterization and Evaluation of Antimicrobial Efficacy and Brine Shrimp Lethality Assay of *Alstonia Scholaris* Stem Bark Extract Mediated ZnONPs. *Biochem. Biophys. Rep.*, 2018, **14**, 69-77. [[CrossRef](#)]
- 13 Yu D.G. Formation of Colloidal Silver Nanoparticles Stabilized by Na<sup>+</sup>-poly (γ-glutamic acid)-Silver Nitrate Complex via Chemical Reduction Process. *Colloids Surf. B: Biointerf.*, 2007, **59**, 171-178. [[CrossRef](#)]
- 14 Sriram M.I.; Kanth S.B.M.; Kalishwaralal K.; Gurnathan S. Antitumor Activity of Silver Nanoparticles in Dalton's Lymphoma Ascites Tumor Model. *Int. J. Nanomed.*, 2010, **5**, 753. [[CrossRef](#)]



© 2021, by the authors. Licensee Ariviyal Publishing, India. This article is an open access article distributed under the terms and conditions of the Creative Commons Attribution (CC BY) license (<http://creativecommons.org/licenses/by/4.0/>).